Journal of
Applied Remote Sensing

Utilization of hyperspectral image optical indices to assess the Norway spruce forest health status

Jan Mišurec
Veronika Kopačková
Zuzana Lhotáková
Jan Hanuš
Jörg Weyermann
Petya Entcheva-Campbell
Jana Albrechtová

SPIE

Utilization of hyperspectral image optical indices to assess the Norway spruce forest health status

Jan Mišurec,[a,b] Veronika Kopačková,[a,b] Zuzana Lhotáková,[c] Jan Hanuš,[d] Jörg Weyermann,[e] Petya Entcheva-Campbell,[f] and Jana Albrechtová[c]

[a]Czech Geological Survey, Klárov 3, Prague 1, 118 21, Czech Republic
E-mail: jan.misurec@geology.cz

[b]Charles University in Prague, Faculty of Science, Department of Applied Geoinformatics and Cartography, Albertov 6, Prague 2, 128 43, Czech Republic

[c]Charles University in Prague, Faculty of Science, Department of Experimental Plant Biology, Viničná 5, Prague 2, 128 44, Czech Republic

[d]The Academy of Sciences of the Czech Republic, Global Change Research Centre, Bělidla 686/4a, Brno, 603 00, Czech Republic

[e]University of Zurich, Remote Sensing Laboratories, Winterthurerstrasse 190, CH-8057, Zurich, Switzerland

[f]NASA Goddard Space Flight Center, Biospheric Sciences Branch, Code 614.4, building 33, Greenbelt, 20771, Maryland

Abstract. The work is concerned with assessing the health status of trees of the Norway spruce species using airborne hyperspectral (HS) data (HyMap). The study was conducted in the Sokolov basin in the western part of the Czech Republic. First, statistics were employed to assess and validate diverse empirical models based on spectral information using the ground truth data (biochemically determined chlorophyll content). The model attaining the greatest accuracy (D_{718}/D_{704}:RMSE $= 0.2055$ mg/g, $R^2 = 0.9370$) was selected to produce a map of foliar chlorophyll concentrations (C_{ab}). The C_{ab} values retrieved from the HS data were tested together with other nonquantitative vegetation indicators derived from the HyMap image reflectance to create a statistical method allowing assessment of the condition of Norway spruce. As a result, we integrated the following HyMap derived parameters (C_{ab}, REP, and SIPI) to assess the subtle changes in physiological status of the macroscopically undamaged foliage of Norway spruce within the four studied test sites. Our classification results and the previously published studies dealing with assessing the condition of Norway spruce using chlorophyll contents are in a good agreement and indicate that this method is potentially useful for general applicability after further testing and validation. [DOI: 10.1117/1.JRS.6.063545]

Keywords: chlorophyll; optical indices; Norway spruce; continuum removal; HyMap, actual physiological status; Sokolov basin, forest management.

Paper 11255 received Nov. 25, 2011; revised manuscript received May 10, 2012; accepted for publication May 11, 2012; published online Jun. 29, 2012.

1 Introduction

Forests play an important role in regulation of the global climate via the global carbon cycle, evapotranspiration, and earth surface albedo.[1,2] Moreover, forests provide humans with the whole range of ecosystem services including provision of food and forest products, regulation of the hydrological cycle, protection of soil resources, etc.[3] Forest health and ecosystem functioning have recently been influenced by anthropogenic activities and their consequences, such as air pollution, surface mining, heavy metal contamination,[4] and other biotic and abiotic stress factors such as pest invasions and soil acidification,[5] which had an especially high effect on central Europe. Therefore, large-scale monitoring of forest health and its methodologies are in the forefront of interest to scientists as well as forest managers. The condition of forests in

0091-3286/2012/$25.00 © 2012 SPIE

Europe is monitored under the International Co-operative Program on Assessment and Monitoring of Air Pollution Effects on Forests (ICP Forests).[6] The monitoring consists of two levels: monitoring Level I provides an annual overview of crown condition (defoliation, discoloration, and damage visible on the trees), soil conditions, and foliar survey (contents of nutrients in soil and foliage);[7] monitoring Level II consists of 11 additional assessments (e.g., tree growth, phenology, litterfall, and others, see http://icp-forests.net/page/level-ii), which provide a better insight into the causes affecting the condition of forest ecosystems and into the effects of various stress factors. Our study aims to contribute to improving regional methods for Level II assessments, as both surveys—remote sensing and foliar chemistry—should be included in the overall evaluation.[8]

Biochemical parameters, such as foliage leaf pigments,[9] nitrogen, lignin, and contents of other polyphenols,[10] reflect and determine physiological processes in plants, such as photosynthetic capacity and net primary production. On the other hand, foliar chemistry also governs other processes in the ecosystem, such as nutrient cycling and litter decomposition.[11] Therefore accurate estimation of the biochemical contents of vegetation is a key factor in understanding and modeling forest ecosystem functions and dynamics. The chlorophyll content is an indicator of leaf photosynthetic activity and can be directly linked to the phenology and health status of plants.[12] Leaf chlorophyll content can be used to detect actual vegetation stress; however, as shown by Ref. 12, the chlorophyll content retrieved from Proba/CHRIS images differs according to the canopy and the leaf architecture of the examined crops. Therefore, at the canopy level, the leaf area index (LAI) and also canopy architecture should be taken into account for a particular canopy. Furthermore, chlorophyll can be used to measure vegetation stress, life stage, productivity, and CO_2 sequestration. Remote sensing of the chlorophyll content has been studied extensively on both the leaf[13,14] and the canopy scales.[15–18]

Many aspects of the physiological state of trees are more or less connected with the concentrations of two main groups of leaf photosynthetic pigments: chlorophylls and carotenoids. Vegetation with a high concentration of chlorophyll is considered to be healthy, as the chlorophyll content is linked to greater light-use efficiency, photosynthetic activity, and carbon dioxide uptake.[19–21] Chlorophyll generally decreases under stress and during senescence.[20] Carotenoids play the main role in the process of incident light absorption, transportation of energy to the reaction center of the photosystems, and heat dissipation of energy in case of high irradiances.[22] The combination of the influences of chlorophylls and carotenoids is thus connected with light-use efficiency.[23] However, higher carotenoid to chlorophyll ratios indicate vegetation stress and senescence.[22,24]

Canopy reflectance depends not only on leaf chemistry but also on vegetation type and function and canopy structure and composition.[16,25] To obtain a spatially explicit vegetation biochemical content, it is necessary to scale leaf-level biochemical measurement to canopy level. Increasing availability of airborne and spaceborne hyperspectral data has enabled the development of accurate methods for scaling of biochemical properties from the leaf to the canopy scale.[26,27]

Currently, there are three remote-sensing approaches used to scale biochemical content from the leaf to the canopy level: (i) the direct extrapolation method, (ii) the canopy-integrated method, and (iii) physical models.[10,28,29] The direct extrapolation and canopy-integration methods rely on statistical analyses to establish a relationship between the targeted biochemical parameter and a spectral parameter (e.g., spectral indices, derivatives).[30,31] The direct extrapolation method (the simplest) is based on the assumptions that all the leaves in the plant have the same biochemical content and only a fine layer of the leaves covers an entire pixel in an image. The relationships between the spectral parameter and the biochemical content are applied directly. Using the canopy-integrated method, the biochemical content is obtained by multiplying the leaf content by the corresponding canopy biophysical parameter (e.g., LAI or biomass[15,29,32]). In addition, new spectral indices taking into account species heterogeneity and non-green canopy components were developed and further tested.[15] Physical methods employ inverted radiative transfer (RT) models (e.g., PROSPECT,[29] LEAFMOD,[28] SAIL,[33] SCOPE[34]) to estimate the biochemical content at the leaf level.[35] RT modeling simulates the transfer of radiation in the canopy by computing the interaction between a plant and solar radiation.[36–38] In comparison with the direct extrapolation and the canopy-integrated approaches, inversion models offer the potential of a more generic approach to quantify the biochemical parameters of vegetation based on spectral data.

The main goal of the study was retrieval of the chlorophyll content and development of a statistical classification method allowing objective assessment of the physiological status of macroscopically undamaged foliage on a regional scale. To simplify the problem, we focused on single-species (Norway spruce) homogenous forests of a similar age and tested only the direct extrapolation and canopy-integrated methods. We did not test physical models at this stage as the computation remains time-consuming and can suffer from ill-posed problems or can lead to a bias in the retrieved biophysical parameters.[39,40]

In the Sokolov area, NW Bohemia, we selected four homogenously covered Norway spruce (*Picea abies L. Karst*) forest stands with trees of similar ages (40 to 60 years) exhibiting no visible symptoms of damage. Although these forests are situated near lignite open-pit mines, they have not been directly affected by intensive mining activities or by the massive air pollution and acid rains in the late 1990s, which were factors in the Krušné Hory Mountains, part of the heavily polluted Black Triangle region. Since 1996, the atmospheric concentrations of SO_2 in Sokolov area have not exceeded 30 μg.m^{-3} and since 2000 have not exceeded 15 μg.m^{-3} on average (data available at Czech Hydrometeorological Institute[41]).

Statistics were employed to analyze the relationship between diverse vegetation indices and other types of spectral transformations [e.g., first derivatives, continuum removal (CR), and band-depth normalizations] and the ground truth data for the foliage sampled in stands of Norway spruce. These diverse approaches were validated, and, as a result, a map of foliar chlorophyll concentrations (C_{ab}) was derived. The C_{ab} values, together with another three optical parameters [the position of the inflection point on the spectral curve in the red-edge part of the spectrum (REP),[42] the photochemical reflectance index,[43] and the Structure Insensitive Pigment Index (SIPI)[44]], were then used to assess the actual health status of the Norway spruce forests.

2 Study Sites

The study was conducted in the Sokolov basin in the western part of the Czech Republic, in a region affected by long-term extensive mining (Fig. 1). The Sokolov basin in the Czech Republic is composed of rocks of Oligocene to Miocene age and is 8 to 9 km wide and up to 36 km long, with a total area of about 200 km^2. It contains 60% volcanic ejecta originating from fissures and volcanic cones and 40% sediments.[45] The average altitude of the study region is about 470 m. Due to the fact that the basin is surrounded by the Krušné Hory Mountains, precipitation is above the average for the Czech Republic, and the local climate in the region belongs among the more extreme conditions, characterized by colder and wetter conditions.

The selected forest stands surround the lignite open pit mines in Sokolov but have not been directly affected by the mining activities. However, the soil in all of the stands exhibits low pH and high heavy metal content. We selected four research sites dominated by mature Norway spruce forests of similar age (Table 1; Erika, Habartov, and Studenec: 40 to 60 years; Mezihorská: 60 to 80 years). The stands were located at a maximum distance of 12 km from the active lignite open pit mines (Fig. 1, Table 1). None of the selected sites showed any severe symptoms of macroscopic damage, and they were all classified as damage class 1 with total crown defoliation not exceeding 25% and average needle retention of 8 to 10 needle age classes.

In relation to soil conditions, we assume that our four study sites are good representatives of the spruce forests in the region. The pH of the study sites (2.53 to 3.31) is slightly below the average for the Czech Republic (3.2) but in accordance with local conditions (3.0).[46] In addition to Norway spruce monocultures, mixed spruce forests (with birch or pine) are characteristic of the region. We selected study sites considering the spatial resolution of the HyMap sensor (5×5 m), and thus homogeneity of spruce canopy was the main criterion for site selection.

3 Data

3.1 *Ground Truth Data*

The source for ground truth data was foliage sampled in the Norway spruce stands. The samples of Norway spruce needles were collected in each forest stand during the ground campaign

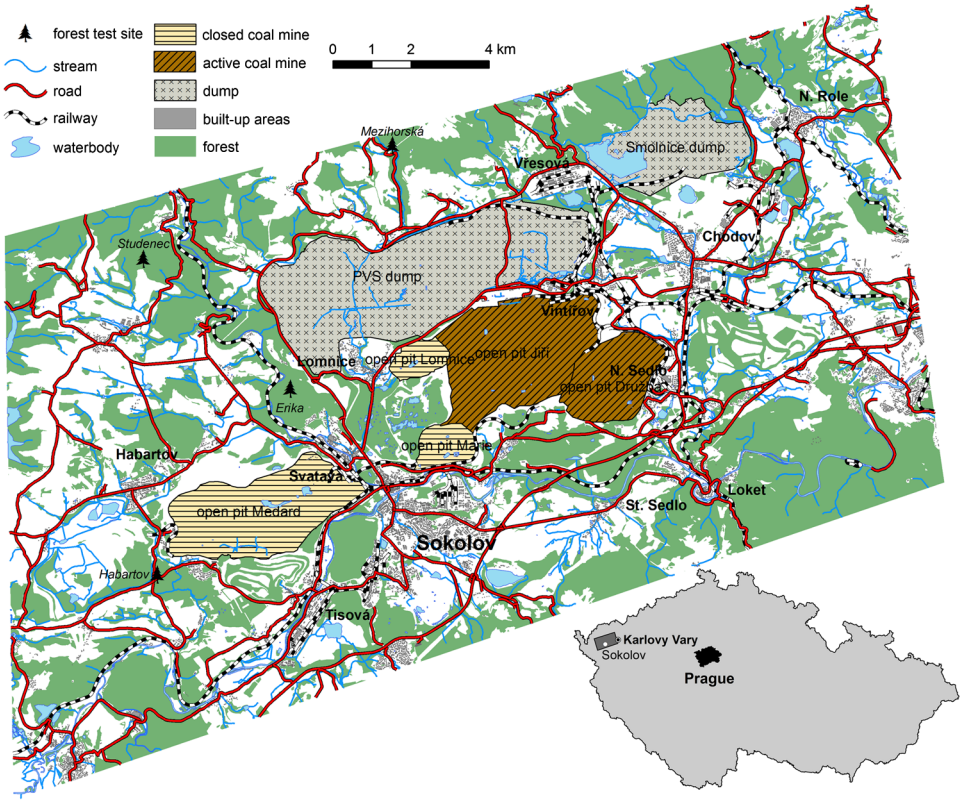

Fig. 1 Scheme of the Sokolov lignite basin with the four selected forest stands covered by homogenous Norway spruce (Picea abies L. Karst.) forests: Erika, Habartov, Mezihorská, and Studenec.

(August 27 to 30, 2009) to define statistical regression models for estimation of canopy chlorophyll content and to validate the obtained statistical models.

At each of the four test sites, 10 to 15 representative trees were selected in clearly definable groups of five (Erika: two groups A and B; Habartov: three groups C, D, and E; Mezihorská: three groups F, G, and H; and Studenec: two groups I and J). Sample branches were taken from the upper and middle portion of the sunlit canopy; the needles age classes were identified, and representative samples of the first- and third-year needles were collected. Two sample sets of the needles were generated: one for pigment determinations and one for dry matter determinations. Each set contained 200 samples (50 trees × two positions in the crown × two age classes (first- and third-year needles).

Photosynthetic pigments (e. g. chlorophyll a, b, and total carotenoids) were extracted following the procedure outlined by Ref. 47. The amounts of photosynthetic pigments were determined spectrophotometrically, using equations published by Ref. 48.

In each forest stand, five representative sampling points were chosen to collect soil samples. Material was collected from four soil horizons (two organic and two lithological horizons, the

Table 1 Norway spruce test sites and their basic characteristics.

Site	Latitude (*N*)	Longitude (*E*)	Elevation (meters above sea level)	Forest age (years)	Distance from the open-pit mines (km)
Erika	50 deg 12'25"	12 deg 36'17"	495	40 to 60	6.4
Habartov	50 deg 09'48"	12 deg 33'28"	477	40 to 60	11.2
Mezihorská	50 deg 15'50"	12 deg 38'17"	678	60 to 80	5.8
Studenec	50 deg 14'09"	12 deg 33'00"	722	40 to 60	8.5

depth of forest floor ranged between 0 and 40 cm). The four horizons have the following characteristics: horizon 1: organic horizon (largely undecomposed); horizon 2: organic horizon (poorly decomposed); horizon 3: mineral, mixed with humus, usually darkened; horizon 4: zone of maximum eluviation of clays and iron and aluminum oxides. The organic material was dried in the air prior to sieving (fraction <2 mm). Ground sub-samples were analyzed for total organic carbon and nitrogen (Perkin Elmer CHN analyzer). In addition, the pH was determined in the laboratory using an ion-selective electrode in 1M KCl solution.

3.2 *High Spectral Resolution Data*

3.2.1 *HyMap airborne hyperspectral data*

The hyperspectral image data was acquired on July 27, 2009, during the HyEUROPE 2009 flight campaign using the HyMap (HyVista Corp., Australia) airborne imaging spectrometer. The HyMap sensor records image data in 126 narrow spectral bands (with full-width half maximum ca. 15 nm) covering the entire spectral interval between 450 to 2500 nm. The resulting ground pixel resolution of the image data was 5 m. To cover the entire area of interest (approx. 15×22 km), nine cloudless flight lines were acquired in the NE-SW direction.

3.2.2 *Supportive ground measurements*

In order to successfully pre-process the hyperspectral data, a supportive calibration and validation ground campaign were organized simultaneously with the HyMap data acquisition. The ground measurements are essential to properly calibrate as well as validate the image data and to enable: (i) atmospheric correction of the airborne hyperspectral images and (ii) retrieving at surface reflectance values for the further verification. The study area was investigated in advance to find the reference targets, which must meet the following conditions: (i) spatial homogeneity for a minimum area of 5×5 image pixels and (ii) natural or artificial nearly Lambertian ground surfaces. Consequently, six appropriate targets with different values of the surface reflectance were chosen, covering the range of reflectivity from ca. 0 up to 70% (water pool, artificial grass, two asphalt plots, concrete, and beach-volleyball court). The hemispherical-conical reflectance factor (HCRF)[49] was measured by an ASD FielSpec-3 spectroradiometer for each reference target. Raw spectroradiometric data were transformed into the HCRF using the calibrated white spectralon panel.

In addition, Microtops II Sunphotometer (Solar Light Comp., USA) measurements were taken approximately every 30 s during the HyMap data acquisition. These data was used for estimation of the actual atmospheric conditions (aerosol optical thickness; water vapor content).

3.2.3 *Hyperspectral image data pre-processing*

The HyMap multiple flight-line data were atmospherically corrected using software (SW) package ATCOR-4 version 5.0,[50] which is based on the MODTRAN[51] radiative transfer model and enables atmospheric correction of the aerial hyperspectral images. The known reflectances of the specific reference target as well as of WV were utilized for fine-tuning of the model, as facilitated by ATCOR-4. The remaining reference targets were used for validation of the corrected image.

The orientation and geometry of the HyMap strips followed the SW-NE orientation of the lignite basin. However, this setting represented an optimal solution from the economic point of view; on the other hand, this setting (relative solar azimuth at the acquisition hour was about 73 deg) caused that the data suffered from strong cross-track illumination and bi-directional reflectance distribution function effects.[52,53] Therefore, in addition to the atmospheric correction, the data had to be further processed to minimize these effects, and semi-empirical nadir normalization using the kernel-based Ross-Li model[54] was performed for all the flight lines.

Direct ortho-georectification was performed using the PARGE software package.[55] Data from the on-board inertial measurement unit/global positioning system unit and digital elevation

model with ground resolution of 10 m were used as the input parameters for the ortho-georectification. Finally, the hyperspectral image data was georeferenced to the UTM 33N (WGS-84) coordinate system. To assess the final accuracy the ortho-rectified HyMap, the product was compared to the very high spatial resolution aerial orthophotos (pixel size = 0.5 m) and a resulting standard positional accuracy of 3.7 m was defined.

Finally, we assessed the radiometric quality of each flight line by calculating the signal-to-noise ratios (SNR).[56] To calculate this parameter, a dark and homogenous surface (deep clean water body) was identified for each flight line and set as a region of interest (ROI). Subsequently, the ratio of the mean radiance and the standard deviation were calculated for each ROI (Table 2). In addition, we employed the minimum noise fraction transformation[57] to assess the level of noise present in each flight line image (Fig. 2). Based on this assessment, we could see that two flight lines (8 and 9) had significantly lower radiometric quality and high amounts of noise, especially flight line number 9 (Table 2), (Fig. 2).

4 Methods

The general workflow of the completed research is outlined in Fig. 3. C_{ab} was determined by testing numerous empirical models utilizing the original (nontransformed) reflectance data as well as its transformed products (see 4.3). Initially we defined the extent of the Norway spruce forests to which the further computation was applied. To create and validate the empirical models, we divided our ground truth data into training and validation datasets. The relationship between the predicted and measured values was described by the linear regression model and the coefficient of determination (R^2 and Rv^2) and root mean square errors (RMSE) were determined. To assess the vegetation health status, we also tested the following indicators: the red-edge part of spectrum (REP),[42] photosynthetic reflectance index,[43] and structure insensitive pigment index (SIPI).[44]

4.1 *Definition of the Norway Spruce Forest Extends*

We focused on homogenous Norway spruce forests, and it was thus necessary to mask out other surfaces. We used a hierarchical classification approach, which we found more efficient than simple supervised classification (Fig. 4). First we identified vegetated and non-vegetated areas using simple threshold classification of the red-edge normalized difference index ($NDVI_{705} = 0.3$).[58] The vegetated surfaces were then classified into grasslands and forest areas using the maximum likelihood classification (MLC) applied to the first five components,

Table 2 Image-derived signal-to-noise ratios (SNR) calculated for the chlorophyll absorption domain bands.

Line	SNR(646 nm)	SNR(660 nm)	SNR(675 nm)	SNR(690 nm)	SNR(704 nm)	SNR(718 nm)
1	46.61	47.50	49.77	43.19	52.98	55.67
2	37.14	33.89	34.17	30.21	28.57	24.55
3	55.01	50.30	47.76	61.63	55.29	48.38
4	36.07	35.57	36.91	34.46	36.26	38.28
5	23.90	24.57	25.34	22.91	23.77	23.89
6	38.15	35.31	36.62	44.82	53.16	40.37
7	49.98	40.20	41.47	36.82	33.42	29.52
8	19.25	19.27	19.09	19.08	20.50	21.83
9	22.03	21.03	19.76	19.46	16.69	16.69

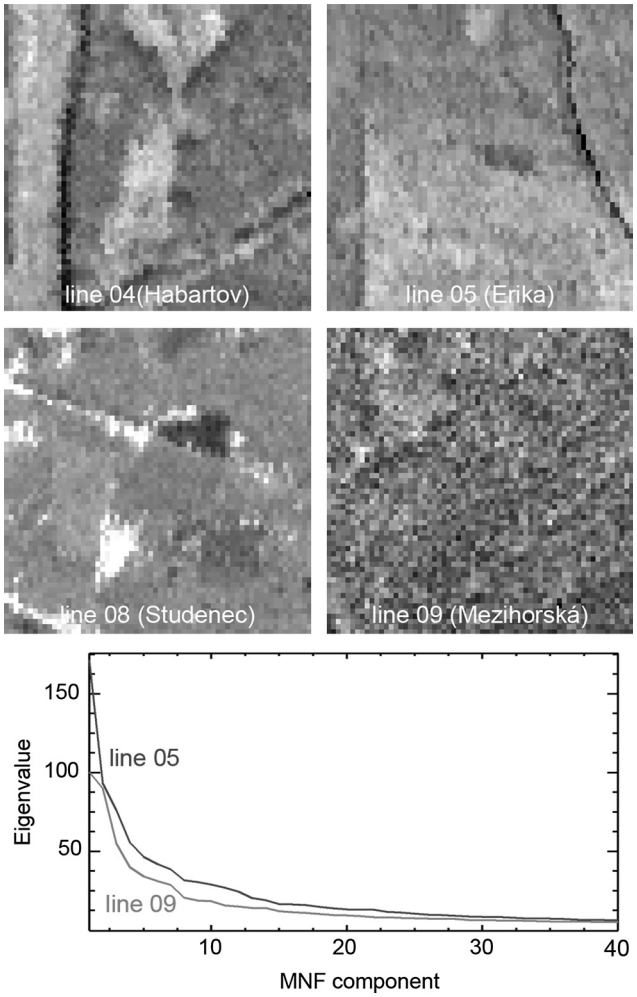

Fig. 2 Upper: The first MNF component of the studied localities, the high amount of noise is visible particularly for flight line No. 9. Bottom: MNF Eigenvalues calculated for the whole flight line images—flight lines numbers 05 and 09. They also show that flight line No. 9 suffers from significantly higher noise levels.

the results from the MNF transformation of the HyMap data. The forests were subsequently divided into coniferous and deciduous by applying the MLC method to the selected spectral ratios (R_{742}/R_{558}, R_{1062}/R_{558}, R_{1652}/R_{558}, R_{2192}/R_{558}).

To classify exclusively the Norway spruce forests, the MNF transformation and MLC were then applied again, this time only to the HyMap reflectance pixels that were previously identified as coniferous. Finally, the resultant classification was filtered using a sieve filter to remove very small clumps of pixels. The derived Norway spruce forest mask was then used for all the following calculations and transformations applied to the HyMap data.

4.2 *Statistical Background*

Although the positions of all the trees in each group were measured by a FieldMap laser rangefinder, it was not possible to distinguish individual tree crowns within the HyMap image data due to the relatively low spatial resolution (5 m). This issue needed to be resolved prior to the empirical modeling as an image pixel value could not be associated with the corresponding ground truth data value. Therefore we defined 10 tree groups as the least circumscribed rectangle defined by a cluster of trees (ROI) (Fig. 5). Then the average ground truth value (the average laboratory chlorophyll content calculated for each tree group) could be directly compared with the average pixel value falling within the defined group (ROI).

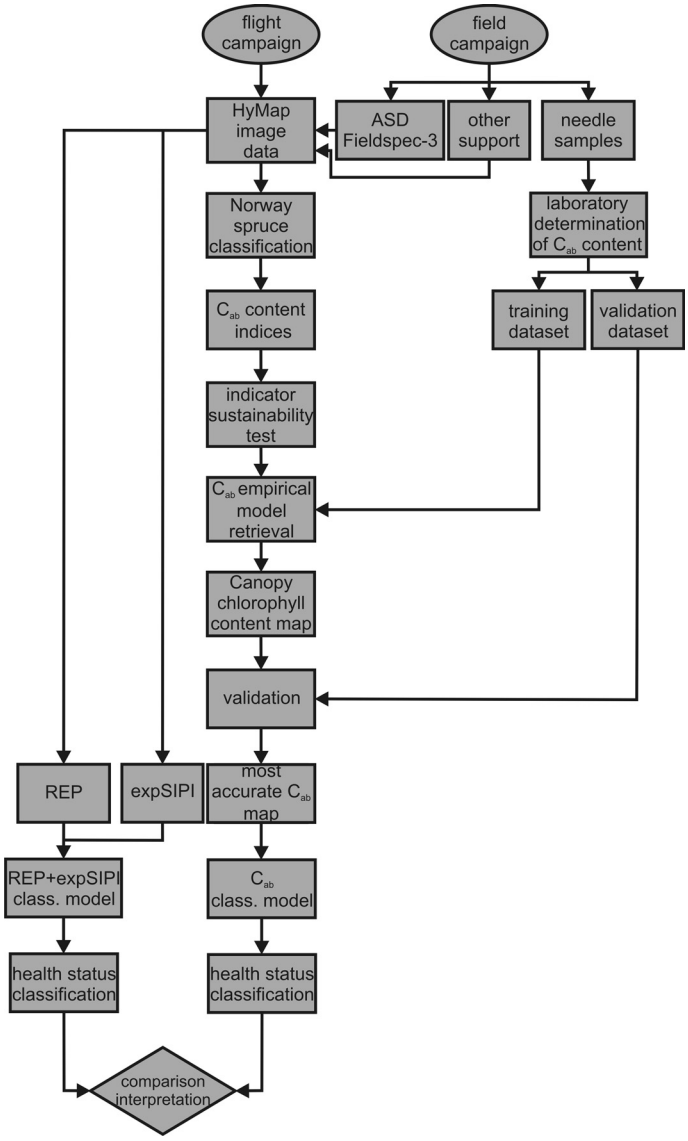

Fig. 3 Data processing workflow.

Basic statistics for each group defined in the following order (Erika: 2 groups A and B; Habartov: 3 groups C, D, and E; Mezihorská: 3 groups F, G, and H; Studenec: 2 groups, I and J, were calculated (Table 3) to ensure the proper definition of training and validation datasets. Studying the data variability within each group and spatial variability within each site, we defined the following two datasets required for further statistical treatment:

- The training dataset that was used to define the regression models: groups A, C, D, F, G, and I.
- The validation dataset that was used to validate the obtained models for C_{ab}: groups B, E, H, and J.

4.3 *Retrieval of the Chlorophyll Content*

For the further empirical modeling of chlorophyll content (C_{ab}), we used the spectral transformations as follows:

- Vegetation indices.
- Stepwise multiple regression (SMR) models.

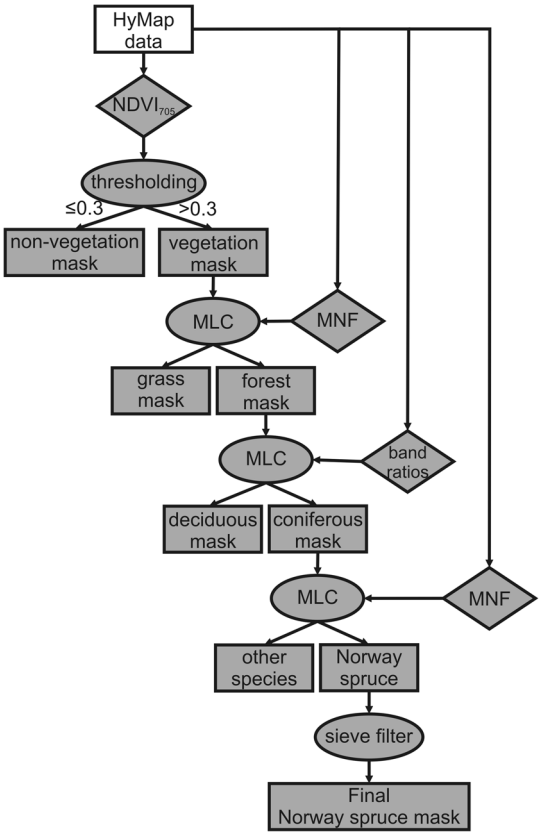

Fig. 4 HyMap data classification workflow. MNF-minimum noise fraction, MLC-maximum likelihood classifier.

- Ratio indices derived from the first-derivative spectra.
- Normalized reflectance models.

4.3.1 *Vegetation indices*

The vegetation indices models are based on the simple linear relationship between the chlorophyll content concentration and the vegetation index. The first group of vegetation indices is based on the (normalized) ratios of a few selected bands. We selected the $NDVI_{705}$[58] and a simple ratio Vogelmann red-edge index (VOG).[59]

Furthermore, we calculated the position of the inflection point of the spectral reflectance curve in red-edge part of the spectra red-edge position (REP)[42] as it allows assessing the

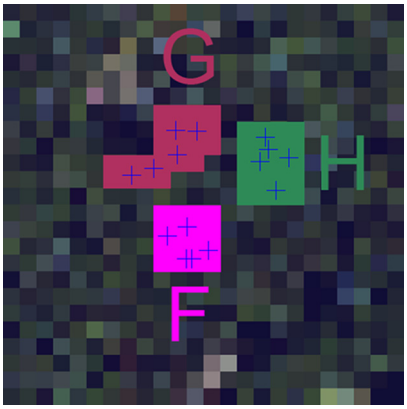

Fig. 5 Examples of the defined ROIs.

Table 3 Description statistics of the laboratory chlorophyll content values.

Group	Locality	Use	C_{ab} (min) [mg/g]	C_{ab} (max) [mg/g]	C_{ab} (mean) [mg/g]	C_{ab} (std) [mg/g]
A	Erika	calibration	1.7260	3.4439	2.7146	0.6251
C	Habartov	calibration	2.1862	3.5375	2.8805	0.4930
D	Habartov	calibration	2.0755	3.1775	2.6008	0.3646
F	Mezihorská	calibration	1.8657	2.3356	2.1417	0.1699
G	Mezihorská	calibration	1.6008	2.3668	2.0292	0.2780
I	Studenec	calibration	2.3670	3.2668	2.9070	0.3121
calibration (the whole dataset)			1.6008	3.5375	2.5456	0.5373
B	Erika	validation	2.0485	3.3826	2.5832	0.4995
E	Habartov	validation	1.8710	2.9022	2.1765	0.3738
H	Mezihorská	validation	1.5004	2.7110	2.3043	0.4260
J	Studenec	validation	2.6293	3.2483	2.8959	0.2321
validation (the whole dataset)			1.5004	3.3826	2.4899	0.4949

shape of the spectral curve in chlorophyll absorption in the red-edge domain. The calculated point separates the convex and concave parts of the spectral curve (in the red-edge part of the spectrum) and lies on the part with the maximum slope. Therefore it also identifies a point where the first derivative of the spectrum exhibits a maximum. To calculate the position of the red-edge inflection point, we used the four-point interpolation technique described in Ref. 60.

Besides the well-known indices, we tested a new index "chlorophyll absorption depth normalized area under curve between 543 and 760 nm ($\mathrm{CADAC}_{543\text{–}760}$)" to retrieve the chlorophyll content of the Norway spruce based on similar principles as the $\mathrm{ANMB}_{650\text{–}725}$ index.[61] The $\mathrm{CADAC}_{543\text{–}760}$ index also utilizes the continuum-removed spectrum and is defined as the area under the reflectance curve between 543 and 760 nm, while each band within this interval is normalized to the maximum depth of the chlorophyll absorption feature (at 675 nm) (Fig. 6):

$$\mathrm{CADAC}_{543\text{–}760} = 0.5 \cdot \sum_{j=1}^{n-1} (\lambda_{j+1} - \lambda_j) \cdot \left(\frac{\mathrm{BD}_{j+1}}{\mathrm{BD}_{675}} + \frac{\mathrm{BD}_j}{\mathrm{BD}_{675}} \right) \tag{1}$$

where: $\lambda_j \ldots \lambda_{n-1}$ refers to the central wavelength between 543 to 760 nm and $\mathrm{BD}_j \ldots \mathrm{BD}_{n-1}$ is the band depth (BD) of continuum removed reflectance.

4.3.2 *Stepwise multiple regression models*

In addition to the vegetation indices, we tested two multivariate approaches that utilize the bands between 543 to 760 nm to estimate the chlorophyll content.[62] We used SMR[63] to construct a model defining a relationship between the chlorophyll content and (i) spectral derivatives: the first derivatives of the image spectra between 543 and 760 nm, (ii) BD normalization: the continuum-removal transformation[64] was applied to the spectrum between 543 and 760 nm, and then the BD of each spectral band was divided by the depth maximum of the chlorophyll absorption (675 nm for the HyMap data).

4.3.3 *Ratio indices derived from the first-derivative spectra*

We used two spectral derivative indices based on the ratios of the transformed (first derivation) reflectance D_{718}/D_{704} and D_{718}/D_{747}.[65]

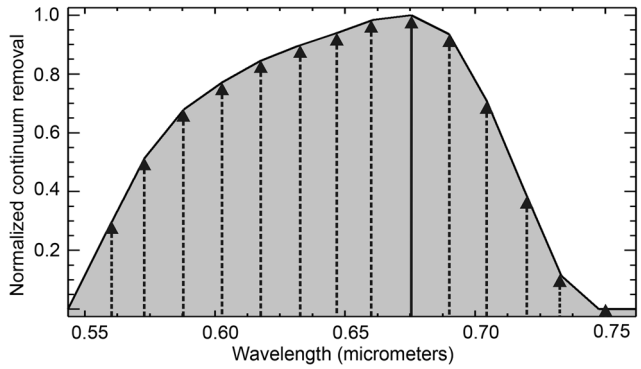

Fig. 6 Chlorophyll absorption and depth normalized area under the curve between 543 to 760 nm ($CADAC_{543–760}$).

4.3.4 *Normalized reflectance models*

Another tested approach was based on the normalization of the reflectance to the reflectance minimum at 675 nm (maximal absorption of the chlorophyll) and to the reflectance maximum at 744 nm.[65]

4.4 *Statistical Assessment of the Relationship Between the Canopy Chlorophyll Content and the Spectral Indices Calculated from the HyMap Data*

To test if there is a linear relationship between the chlorophyll content determined in the laboratory for the collected needle samples and the spectral indices derived from the HyMap data, we calculated Pearson's correlation coefficient (see Sec. 5.1) using the training dataset of the group trees (A, C, D, F, G and I). All the independent variables (see 4.3) as well as the dependent variable (laboratory chlorophyll content, C_{ab}) have passed the Shapiro-Wilk normality test[66] (p-value > 0.05) and proved to have normal distributions (Table 4).

After the normal distribution of all the variables was demonstrated, we could test whether the value of the correlation coefficient was large enough to reject the zero-value hypothesis stating the correlation coefficient is equal to 0. By rejecting this hypothesis, we demonstrated that the spectral indicators and the chlorophyll content are not independent. The confidence level was set at 98.5%. Following the statistical testing described above, the linear regression models were then applied to the spectral indices data to predict the canopy chlorophyll content.

Using the training dataset (tree groups A, C, D, F, G, and I), the coefficient of determination (R^2) between each spectral index and the C_{ab} content was calculated (Table 5), describing the amount of data variability explained. The validation dataset (tree groups B, E, H, and J) was then used to validate the accuracy and consistency of the chlorophyll prediction models by calculating the RMSE and coefficients of determination of predicted versus measured C_{ab} values (Rv^2) (Table 6).

4.5 *Vegetation Health Status Classification Method*

The main aim of the study was to develop a statistical method allowing qualitative classification of the forest stands based on their health status. We selected four indicators of vegetation health that are based on the plant/forest spectral property:

1. Total canopy chlorophyll content (C_{ab}) (D_{718}/D_{704})[65]
2. Position of the inflection point of the spectral curve in the red-edge part of spectrum (REP)[42]
3. Photosynthetic reflectance index (PRI)[43]
4. Structure insensitive pigment index (SIPI)[44]

Table 4 Results of the Shapiro-Wilk normality test for chlorophyll content (C_{ab}) values (laboratory determined) and the spectral transformation image products (p-value—significance; W—Shapiro-Wilk test statistic).

Variable	p-value	W
C_{ab}	0.1862	0.8936
$NDVI_{705}$	0.4348	0.9287
VOG	0.4745	0.9327
REP	0.1667	0.8893
$CADAC_{543–760}$	0.3900	0.9238
SMR spectral derivative model	0.7879	0.8992
Continuum removal BD normalization model	0.1877	0.8939
D_{718}/D_{701}	0.6273	0.9465
D_{718}/D_{747}	0.7430	0.9563
N_{690}	0.0599	0.8512
N_{704}	0.2197	0.9001
N_{718}	0.2393	0.9035
N_{733}	0.5920	0.9435

Table 5 Training dataset: Pearson's correlation coefficient (r_{xy}), coefficient of determination (R^2) and the t-test results.

Spectral indicator	r_{xy} (Pearson)	Critical value ($\alpha = 0.05$)	t	R^2
$NDVI_{705}$	0.8517	2.776	3.2509	0.7254
VOG	0.9085	2.776	4.3494	0.8255
REP	0.9397	2.776	5.4932	0.8830
$CADAC_{543–760}$	0.8899	2.776	3.9026	0.7920
SMR spectral derivative model[a] (D_{632}, D_{661}, D_{544})	−0.9225 −0.6931 0.2558	X	X	0.99998
Continuum removal BD normalization model (R_{CR}norm705)	0.9398	2.776	5.5003	0.8831
D_{718}/D_{704}	0.9555	2.776	6.4782	0.9131
D_{718}/D_{747}	−0.8807	2.776	3.7186	0.7756
N_{690}	−0.9013	2.776	4.1612	0.8124
N_{704}	−0.9306	2.776	5.0847	0.8660
N_{718}	−0.9563	2.776	6.5413	0.9146
N_{733}	−0.8914	2.776	3.9337	0.7946

[a]partial correlation coefficients between canopy chlorophyll content and each variable of the multivariate regressions.

Table 6 Validation dataset: Validation of the total canopy chlorophyll content retrieved from the HyMap image data. Root mean square error (RMSE), Rv^2—coefficient of determination of the predicted versus measured values of the chlorophyll content.

Spectral indicator	RMSE (mg/g)	Rv^2
$NDVI_{705}$	0.2278	0.8960
VOG	0.2269	0.9340
REP	0.3840	0.9050
$CADAC_{543-760}$	0.3395	0.9114
SMR spectral derivative model(D_{632}, D_{661}, D_{544})	0.7962	$1 \cdot 10^{-5}$
continuum removal BD normalization model (R_{CR}norm705)	0.2832	0.9328
D_{718}/D_{704}	0.2055	0.9370
D_{718}/D_{747}	0.2456	0.9880
N_{690}	0.4305	0.8254
N_{704}	0.2833	0.9293
N_{718}	0.2664	0.9440
N_{733}	0.2736	0.9905

The canopy chlorophyll content was estimated using the empirical model that yielded the best results after the validation (see Results, part 5.1).

The amount of green biomass and canopy chlorophyll content primarily determine the position of the inflection point of the spectral curve in the red-edge region. Increasing chlorophyll concentration causes broadening of the major chlorophyll absorption feature around 675 nm and thus causes a shift in the inflection point towards longer wavelengths.[67–71] On the other hand, vegetation stress (e.g., the presence of heavy metals in the soil) might cause a shift in the inflection point to shorter wavelengths.[72] Therefore we also included REP (described in 4.3.1) in the further statistics, as it can serve as an indicator of the vegetation stress.[42,71,73,74]

The PRI was originally defined by Ref. 43 and proposed as an indicator of the de-epoxidation of the carotenoids—xanthophyll pigments; they are related to light-absorption mechanisms and closely linked with light use efficiency and carbon dioxide uptake;[43,75] and Refs. 76 and 77 propose to use this index as an indicator of water stress.

The SIPI was designed by Ref. 44 to maximize the sensitivity of the index to the ratio of bulk carotenoids to chlorophyll while decreasing sensitivity in the canopy structure. Due to the relative low dynamic range of the SIPI values, we used its exponential transformation (expSIPI) in further analysis.

We must emphasize that, except for the canopy chlorophyll content, none of these indices give direct quantitative information on any particular vegetation biochemical parameter. Instead, they are intended to map only relative amounts, which can be further interpreted in terms of the condition of the ecosystem.

The statistical relationship between the estimated canopy chlorophyll content and the selected indicators (e.g., REP, PRI, and SIPI) was assessed (Fig. 7). We found that the value of PRI did not change much for the Norway spruce in the entire area of interest and thus didn't show high enough variability. In addition, the direct relationship of PRI to the chlorophyll content was also relatively weak. Therefore we decided to exclude the PRI index from further investigations.

The values of the three selected indices were transformed into standardized z-scores (Table 7) to ensure their comparability and independence of their physical dimensions (units).

Z-scores generally express how far from the mean the particular value is in terms of the standard deviations (σ). Two products were created using the obtained normalized z-score

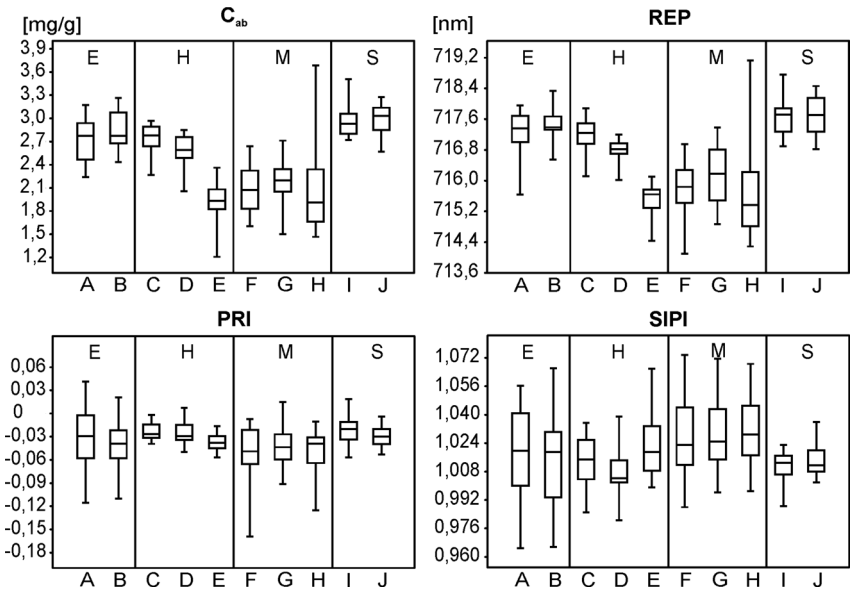

Fig. 7 The selected indicator variability within the studied test sites/groups of trees. C_{ab}—content of chlorophyll $a + b$, REP—position of the inflection point of the spectral curve in the red-edge part of the spectrum; photochemical reflectance index (PRI); structure insensitive pigment index (SIPI); A through *J*, 10 groups of five sampled trees.

values. First the map of chlorophyll content was classified into five classes defined by the following threshold values (Fig. 8):

Class 1: values < mean − 1.0σ
Class 2: mean − 1.0σ < values < mean − 0.5σ
Class 3: mean − 0.5σ < values < mean + 0.5σ
Class 4: mean − 0.5σ < values < mean + 1.0σ;
Class 5: values > mean + 1.0σ.

In addition to the classified chlorophyll content map, we created another raster product that combined the information from both indicators REP and expSIPI. REP has the same directly proportional relationship with the vegetation health as the chlorophyll content, and REP was therefore classified identically. On the other hand, expSIPI needed to be classified in the reverse order as the higher values reflect higher carotenoid-to-chlorophyll contents and thus worse vegetation health (in this case Class 1 was calculate as values > mean + 1.0σ, . . . , Class 5 as values < mean − 1.0σ). To create the final raster combining the information from REP and expSIPI, they were both summarized and one raster ranging from 2 to 10 was obtained. These values were finally linearly reclassified into the 1 to 5 range to make this output comparable with the C_{ab} raster (Fig. 9). As a result, in both maps (C_{ab} and REP + exp SIPI) the Class 1 indicates worse health status for the trees without visible damage symptoms and Class 5 represents the values indicating the healthiest trees.

Table 7 Threshold values of selected indicators used for the further health status assessment. Mean (μ) and standard deviation (σ).

Health status indicator	-1.0σ	-0.5σ	$+0.5\sigma$	$+1.0\sigma$	μ
C_{ab}[mg/g]	1.914	2.219	2.828	3.132	2.523
REP [nm]	715.508	716.107	717.306	717.905	716.706
expSIPI	2.683	2.724	2.806	2.847	2.765

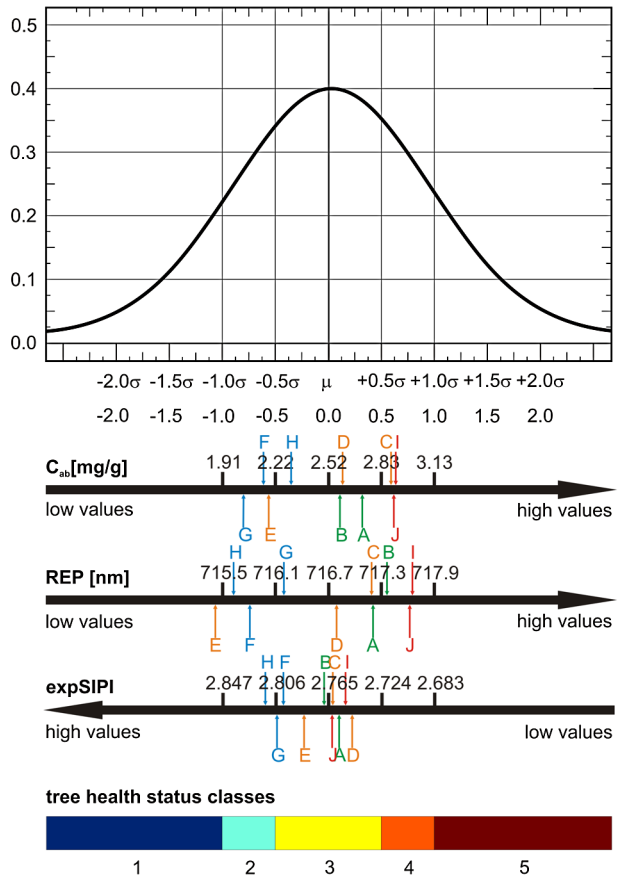

Fig. 8 Scheme showing how the suggested statistical method was constructed. The *z*-normalized values of all three selected indicators are classified into Classes 1 through 5 using the standard deviation (σ) classification method. The studied groups of trees (A through *J*) are projected on an absolute scale for each indicator. The colors correspond with the locations of the studied groups of trees (green A, $B =$ Erika; orange C, D, $E =$ Habartov; blue H, $G =$ Mezihorská; and red I, $J =$ Studenec). C_{ab}—content of chlorophyll $a + b$, REP—Position of the inflection point of spectral curve in red-edge part of spectrum, expSIPI—exponentially transformed structure insensitive pigment index.

5 Results and Discussion

5.1 *Validation and Prediction of the Canopy Chlorophyll Content (C_{ab})*

In both multivariate approaches, the SMR spectral derivative and the continuum removal BD normalization models, the null hypothesis was tested employing SMR. As a result, three different derivative variables (the derivative of the bands with central wavelengths 632, 661, and 544 nm) and only one normalized band ($R_{\mathrm{CR\,norm}705}$) passed this test and where further used (Table 5).

Using the training dataset (A, C, D, F, G, and I), we obtained the models that all attained r_{xy} high enough to pass the initial *t*-test (Table 5).

For the validation dataset (groups B, E, H, and J), the statistical parameters, Rv^2 and RMSE (Table 6), were used to test how well the linear models can predict the chlorophyll content, and the image average values were compared with the average values of the chlorophyll content obtained in the laboratory (ground truth).

In general, we obtained rather high coefficients of determination for the linear models calculated between the tested spectral indices and the ground truth dataset (canopy chlorophyll content) on both the training and the validation datasets (R^2, Rv^2). These results confirmed the assumption of a strong dependence between the selected spectral indicators and the canopy

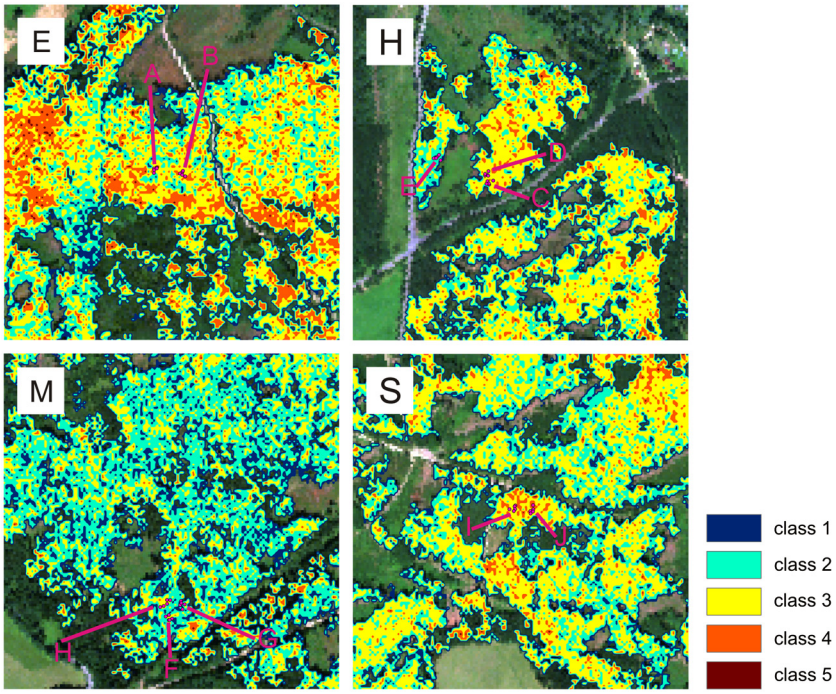

Fig. 9 Statistical classification of the Norway spruce health status by integrating the C_{ab}, REP, and expSIPI. E = Erika; H = Habartov; M = Mezihorská; S = Studenec study sites; A through J; 10 defined tree groups. Color scale 1 through 5—health status classes for the trees without visible damage symptoms; 1 = the worst and 5 = the best result (see Fig. 8).

chlorophyll contents. The scatterplots between ground (laboratory) chlorophyll content value and selected image derived spectral indices are shown in Fig. 10.

For the training dataset (Table 5), the highest correlation coefficients (strongest linear relationship) were obtained for the normalized reflectance (N_{718}) and the derivative ratio (D_{718}/D_{704}) models. The weakest correlation was found for the NDVI_{705} index. The strong negative correlations between the canopy chlorophyll content and the normalized reflectances (N_{690}, N_{704}, N_{718}, and N_{733}) are in accordance with the theoretical background. The higher the chlorophyll concentration, the higher is the absorption of radiation and the lower is the observed reflectance. SMR analysis found a valid result only for the multiple linear regression of spectral derivatives. For this particular case, we were able to calculate only the partial correlation coefficients between each independent variable (spectral index) and the dependent variable chlorophyll content (chlorophyll content). Therefore the general coefficient (r_{xy}) was not defined for this model.

Comparing R^2 (Table 5) to RMSE (Table 6) indicates that the model exhibiting the highest R^2 does not necessarily give the best result. This can be demonstrated on the example of the multiple linear model calculated from the spectral derivatives. Despite the very high value of $R^2 (R^2 = 0.99998)$, the model has the highest RMSE ($\mathrm{RMSE} = 0.7962$ mg/g, relative $\mathrm{RMSE} = 32\%$). We assume this is due to the rather high noise level, which was multiplied by calculating the first derivatives from the image spectrum.

The variability and the dynamic range of the predicted values for the chlorophyll contents were compared with the ground truth dataset using box plot diagrams. The box plots constructed for the predicted C_{ab} values (D_{718}/D_{708}) and the ground truth C_{ab} data (Fig. 11) exhibit good agreement for the Studenec and Erika sites. In contrast, a worse match was found for the Mezihorská test site, where extremely high variability of the predicted values can be observed. This can be explained by the low radiometric quality of the HyMap line (line No. 9) where the site is located. This particular line No. 9 suffers from a very high noise level compared with the other HyMap lines acquired in 2009 (see Chap. 3, Table 2, Fig. 2).

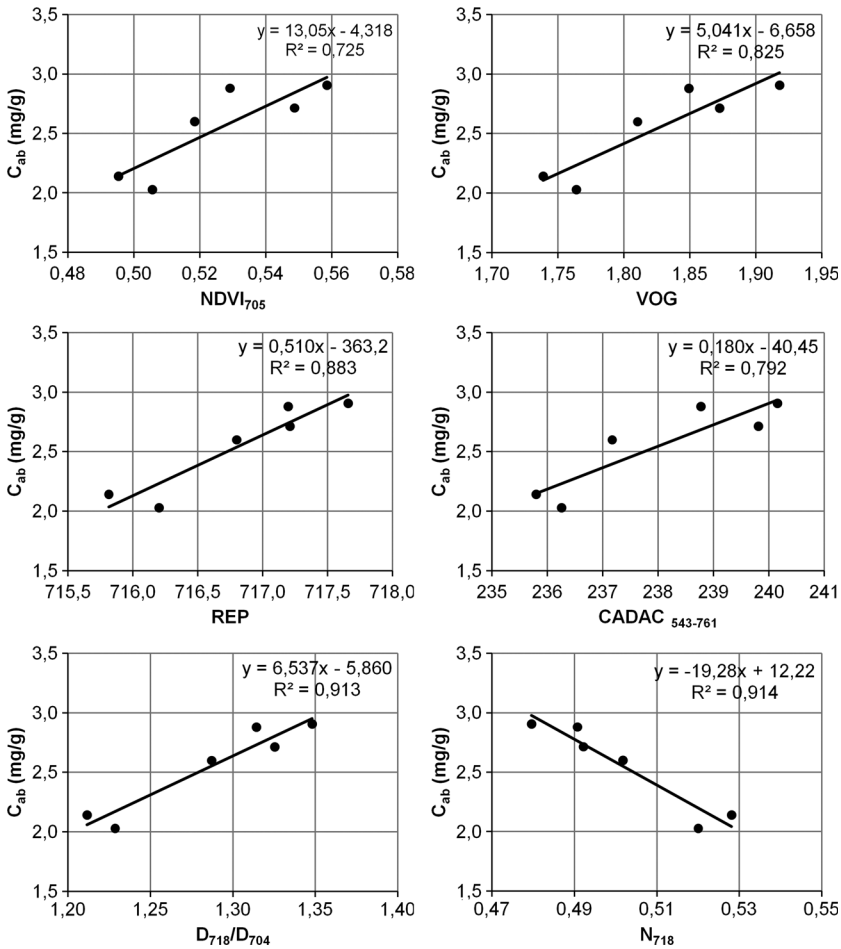

Fig. 10 Scatterplots between ground (laboratory) measured chlorophyll content and selected image derived hyperspectral indices.

The best result taking in account R^2, Rv^2, and RMSE was obtained using the model based on the D_{718}/D_{708} ratios ($R^2 = 0.9131$, $Rv^2 = 0.9370$, $\mathrm{RMSE} = 0.2055$ mg/g, and relative $\mathrm{RMSE} = 8\%$). Therefore the D_{718}/D_{708} model was applied to the all HyMap image data (lines 1 through 9) to retrieve the map of the canopy chlorophyll content (Fig. 12). This output was further used to assess the canopy health status.

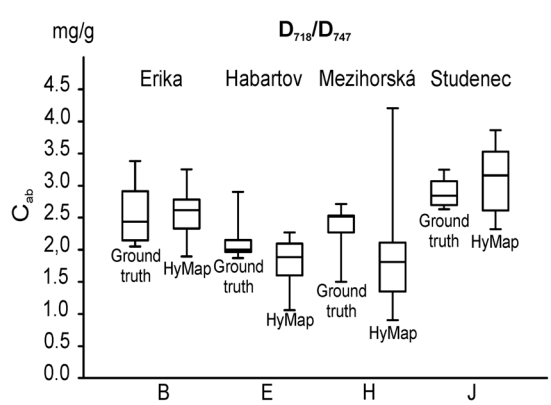

Fig. 11 Box plots of the measured (ground truth) and the predicted (HyMap) canopy chlorophyll contents for the derivative ratio index (D_{718}/D_{708}—content of chlorophyll $a+b$ (g of pigment related to dry mass).

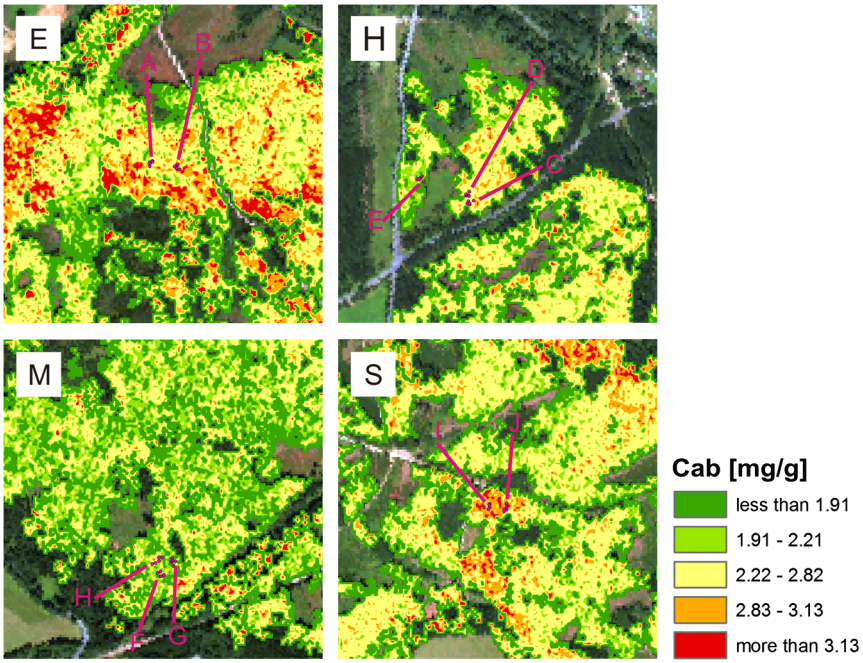

Fig. 12 Map of the Norway spruce canopy chlorophyll content derived by applying the D_{718}/D_{704} regression model. E = Erika; H = Habartov; M = Mezihorská; S = Studenec. C_{ab}—content of chlorophyll $a + b$ (mg of pigment related to dry mass); A through J—10 groups of five sampled trees.

5.2 *Assessment of the Norway Spruce Health Status*

Two statistical scenarios, C_{ab} and REP + exp SIPI, were tested to assess and classify the Norway spruce health status (see Chap. 4.5). Both scenarios were applied to all the pixels classified as homogenous Norway spruce forest in the HyMap image data (lines 1 through 9) (Fig. 9).

In both cases, C_{ab} and REP + exp SIPI, the frequency histograms (Figs. 13 and 14) show rather symmetrical distribution that is close to the Gaussian normal distribution. However, the histograms computed for each test site (Erika, Habartov, Mezihorská, and Studenec) show significant asymmetries. At the Erika site, we can identify slight asymmetry toward the higher-class values, indicating the higher frequencies of average and above-average values. On the other hand, for the Habartov site we can observe slight asymmetry toward the lower-class numbers, indicating the higher frequencies of average and below-average values. For the Mezihorská site, a very strong asymmetry can be observed. The majority (almost 75%) of the pixels were classified into the Classes 1 and 2, while Classes 4 and 5 have very low frequencies. The opposite situation can be observed for the Studenec site, where a strong asymmetry toward the high classes can be observed.

Comparing the two tested classification scenarios (C_{ab} and REP + exp SIPI), the C_{ab} method shows higher data variability. The C_{ab} scenario has higher frequencies of extreme values (Class 1 and Class 5) in contrast with the REP + exp SIPI scenario, where the values are more frequently classified in the average Class 3. This can be explained by the higher variability of the C_{ab} values compared with the expSIPI values.

The laboratory analysis of the Norway spruce needles, collected during the project described in Ref. 61, indicated that higher needle chlorophyll content is not automatically connected with a better health status. Therefore the chlorophyll content itself cannot be the only indicator of damage to the Norway spruce. To take in account this fact, the expSIPI index was used as a correcting factor in the selected model. If the Norway spruce stands have very high C_{ab} and REP values, and the expSIPI values don't indicate any health damage, the pixels fall into average Class 3 instead of being classified in Class 4 or 5.

All the studied sites exhibited soil solution pH values under 3.5 (Table 8), which correspond to low pH threshold for forest soils in the Czech Republic.[46] We assume that soil acidity is the

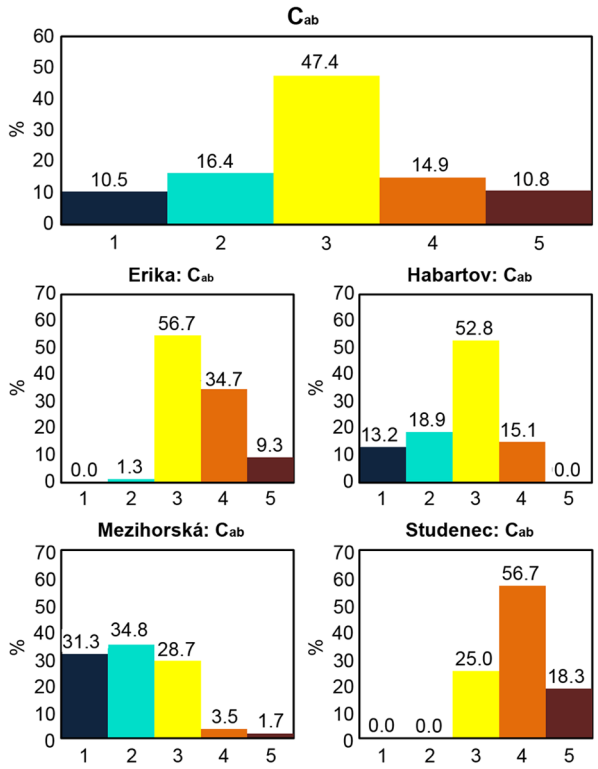

Fig. 13 Relative frequencies (%) of the Norway spruce health status classes obtained for the C_{ab} classification scenario. The entire Sokolov lignite basin area (top) and the individual sites Erika, Habartov, Mezihorská, and Studenec (below).

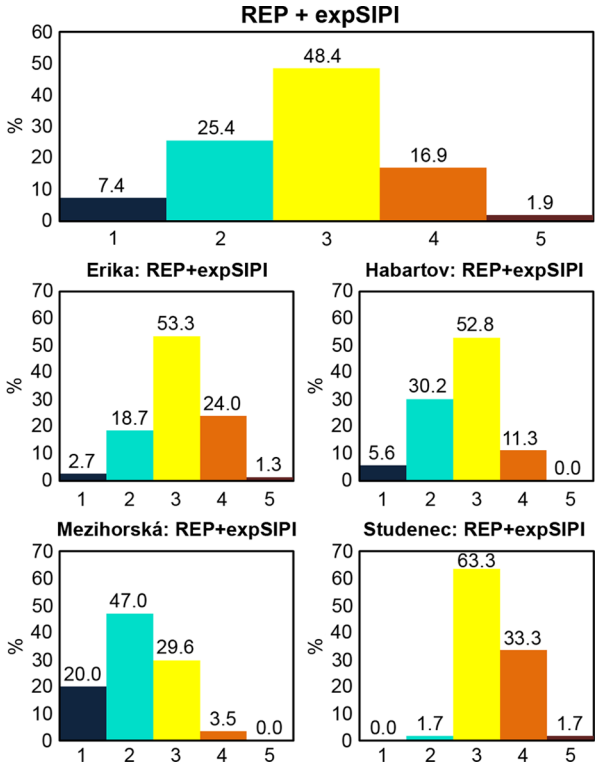

Fig. 14 Relative frequencies (%) of the Norway spruce health status classes obtained by the statistical scenario REP + expSIPI. The entire Sokolov lignite basin area (top) and the individual sites Erika, Habartov, Mezihorská, and Studenec (below).

Table 8 The soil solution pH (in KCl) and $C:N$ ratio for the two organic top horizons. One-way ANOVA.

	pH (KCl)			$C:N$ ratio		
Site	Upper horizons	Lower horizons	Both horizons	Upper horizons	Lower horizons	Both horizons
Erika	2.55^{bb}	2.50^{db}	2.53^{db}	28.06^{aca}	27.10^{ns}	28.40^{ns}
Habartov	3.18^{adb}	3.43^{ab}	3.31^{ab}	26.68^{ba}	31.80^{ns}	29.24^{ns}
Mezihorská	2.87^{cb}	2.76^{cb}	2.81^{cb}	28.65^{abca}	27.24^{ns}	27.65^{ns}
Studenec	3.33^{ab}	2.99^{bb}	3.16^{bb}	29.70^{aa}	26.80^{ns}	27.73^{ns}

Different letters indicate significant differences between sites according to Tukey-Krammer multiple comparison test[78]
[a]Significant difference at 0.05.
[b]Significant difference at 0.01.

main stress factor in the studied locality. This finding is supported by the fact that Central Europe and Denmark were considered to be the areas with the highest exceeding of limits for soil acidification indicators, pH and base cations-to-Al ratios in 2010.[79] Soil conditions, especially nutrient availability and balance, determine the physiological status of forest trees. Nutrient imbalances and deficiencies may result in increased susceptibility to a number of stress factors, such as weather extremes or pest invasions.[79] Thus determination of the health status of trees should include evaluation of numerous parameters and should also take into account other factors such as soil pH and the base cations-to-Al ratios, used to estimate the risk of damage to the vegetation from acidified soil (ICP Forests Executive Report, 2010). High values of the organic horizon $C:N$ ratios (above 22) also imply the possibility of lower nitrification[11] and thus slower nutrient turnover or misbalance.

6 Conclusions

According to the ICP Forest methodologies, the main indicators for forest health assessment at Level I consists in evaluation of crown defoliation and foliage discoloration; however several limitations of these indicators have been discussed recently.[6] Although the chlorophyll content could serve as a relevant quantitative forest health indicator, it is not included either in the foliage chemistry indicators of the ICP Forest manual[80] or in the US Forest Service's Forest Inventory and Analysis program.[81] This could be explained by the fact that large-scale assessment of the chlorophyll content could be problematic due to laboriousness and high costs of the needle sampling and biochemical analyses. At the present time, hyperspectral technologies provide an opportunity to retrieve a reliable continuous chlorophyll model while requiring only a reasonable number of samples.

Although the chlorophyll content in foliage is quite often declared to be an indicator of plant physiological status,[82] the uniform classification of chlorophyll contents for Norway spruce needles is not yet very well established. To date, no fixed threshold values of needle chlorophyll content for determination exact classes of forest health status exists. The actual chlorophyll content in the needles of coniferous trees depends on the local and microclimatic conditions, including geographical factors such as latitude and altitude.[83] Particularly the altitude correspond with a combination of several environmental factors, such as irradiance,[17,18] temperature, water, and nutrient availability, which are all factors that influence the chlorophyll content in foliage.[83,84] Oleksyn et al.[83] reported that seedlings of high-altitude Norway spruce populations in colder regions contained higher chlorophyll concentrations in needles than trees at low elevations. According to Ref. 85, the chlorophyll content in needles of healthy mature (60 years and older) Norway spruce (altitude 840 m) ranges between 2.2 to 2.7 mg per gram of dry mass and other authors state even higher chlorophyll contents: 3.21 ± 0.30 mg per gram of dry mass (altitude 400 m)[62] or 4.30 ± 1.06 mg per gram of dry mass (altitude 700 m).[86] Therefore

it is necessary in each case to adjust the threshold values of the chlorophyll content to local conditions. We assume that our model could be applied to other spruce or coniferous species, but at least minimal ground truth calibration and laboratory analyses of pigment contents are advisable. It appears that local environmental conditions affect the chlorophyll content even more strongly than the difference between two spruce species. According to Barsi et al.,[84] the difference in chlorophyll content in needles of early succession black spruce (1.6 mg per gram of dry mass) and late succession red spruce (1.44 mg per gram of dry mass), both grown under the same controlled conditions, was on average only 10%.

We evaluated the numerous approaches to determine the chlorophyll content empirically. The individual models were statistically assessed using the ground truth training/validation datasets and the best model based on the spectral derivative ratio (D_{718}/D_{704}, RMSE $= 0.2055$ mg/g, $R^2 = 0.9370$) was chosen to estimate the chlorophyll (C_{ab}) content for the Norway spruce species using the HyMap multiflight line data. Then we developed a new statistical method to assess the physiological status of macroscopically undamaged foliage of Norway spruce. As the chlorophyll content alone may not correspond sufficiently well to the physiological/health status, the suggested method utilizes three indicators (C_{ab}, REP, expSIPI). Thus the suggested method takes in account the two major biochemical parameters that are closely connected with photosynthetic functions (chlorophylls and carotenoids), and it allows assessing of the vegetation stress in a more objective way.

Based on our z-score classification of the needle chlorophyll content, the medium health status class of trees lacking visible damage symptoms (Class 3, chlorophyll content 2.22 to 2.83 mg per gram dry mass) corresponds well with the chlorophyll values reported by Ref. 84. This accordance suggests the possibility of the general applicability of our model after further testing and validation.

Acknowledgments

The research is being undertaken as part of a larger HYPSO scientific research project within the framework of grant No. 205/09/1989 funded by the Czech Science Foundation. Many thanks belong to Dr. Jan Frouz for his technical support of the field campaign and to all the students who participated in sample collection.

References

1. R. B. Jackson et al., "Protecting climate with forests," *En. Re. Lett.* **3**(4), 044006 (2008), http://dx.doi.org/10.1088/1748-9326/3/4/044006.
2. G. B. Bonan, "Forest and climate change: forcing, feedbacks and their climate benefits of forests," *Science* **320**(5882), 1444–1449 (2008), http://dx.doi.org/10.1126/science.1155121.
3. R.Hassan and N. Scholes, Eds., *Ecosystems and Human Well-being: Current State and Trends*, p. 815, Island Press, Washington, DC (2005).
4. J. C. Aznar et al., "Lead exclusion and copper translocation in black spruce needles," *Water Air Soil Poll.* **203**(1–4), 139–145 (2009), http://dx.doi.org/10.1007/s11270-009-9997-8.
5. P. Šebesta et al., "Acidification of primeval forests in the Ukraine Carpathians: vegetation and soil changes over six decades," *Forest Ecology Manag.* **262**(7), 1265–1279 (2011), http://dx.doi.org/10.1016/j.foreco.2011.06.024.
6. J. Johnson and M. Jacob, "Monitoring the effects of air pollution on forest condition in Europe: is crown defoliation an adequate indicator?" *iForest* **3**, 86–88 (2010), http://dx.doi.org/10.3832/ifor0538-003.
7. Large scale forest condition. [on-line], http://icp-forests.net/page/largescale-forest-condition.
8. ICP forest assessment—level II. [on-line], http://icp-forests.net/page/level-ii.
9. S. L. Ustin et al., "Retrieval of foliar information about plant pigment systems from high resolution spectroscopy," *Re. Sens. Envir.* **113**, S67–S77 (2009), http://dx.doi.org/10.1016/j.rse.2008.10.019.
10. R. F. Kokaly et al., "Characterizing canopy biochemistry from imaging spectroscopy and its application to ecosystem studies," *Re. Sens. Envir.* **113**, S78–S91 (2009), http://dx.doi.org/10.1016/j.rse.2008.10.018.

11. S. V. Ollinger et al., "Regional variation in foliar chemistry and N cycling among forests of diverse history and composition," *Ecology* **83**(2), 339–355 (2002), http://dx.doi.org/10.2307/2680018.
12. J. S. Delegido et al., "Estimating chlorophyll content of crops from hyperspectral data using a normalized area over reflectance curve (NAOC)," *Inter. J. App. Earth Ob. Geoinfo.* **12**(3), 165–174 (2010), http://dx.doi.org/10.1016/j.jag.2010.02.003.
13. D. H. Card, D. L. Peterson, and P. A. Matson, "Prediction of leaf chemistry by the use of visible and near infrared reflectance spectroscopy," *Re. Sens. Envir.* **26**(3), 123–147 (1988), http://dx.doi.org/10.1016/0034-4257(88)90092-2.
14. D. L. Peterson et al., "Remote sensing of forest canopy and leaf biochemical contents," *Re. Sens. Envir.* **24**, 85–108 (1988), http://dx.doi.org/10.1016/0034-4257(88)90007-7.
15. A. Gitelson et al., "Remote estimation of canopy chlorophyll content in crops," *Geophys. Re. Lett.* **32**, 4–7 (2005), http://dx.doi.org/10.1029/2005GL022688.
16. B. Datt, "A new reflectance index for remote sensing of chlorophyll content in higher plants: tests using eucalyptus leaves," *J. Plant Phy.* **154**(1), 30–36 (1999), http://dx.doi.org/10.1016/S0176-1617(99)80314-9.
17. A. D. Richardson, G. P. Berlyn, and T. G. Gregoire, "Spectral reflectance of Picea rubens (Pinaceae) and Abies balsama (Pinaneae) needles along an elevational gradient, MoosilaukeMt., New Hampshire," *1. Am. J.Botany* **88**(4), 667–676 (2001), http://dx.doi.org/10.2307/2657067.
18. A. D. Richardson, J. B. Reeves, and T. G. Gregoire, "Multivariate analyses of visible/near infrared (VIS/NIR) absorbance spectra reveal underlying spectral differences among dried, ground conifer needle samples from different growth environments," *New Phytologist* **161**(1), 291–301 (2004), http://dx.doi.org/10.1046/j.1469-8137.2003.00913.x.
19. P. J. Kramer, "Carbon dioxide concentration, photosynthesis and dry matter production," *BioScience* **31**(1), 29–33 (1981), http://dx.doi.org/10.2307/1308175.
20. G. A. Blackburn, "Hyperspectral remote sensing of plant pigments," *J. Exper. Botany* **58**(4), 855–867 (2007), http://dx.doi.org/10.1093/jxb/erl123.
21. C. Wu et al., "Estimating chlorophyll content from hyperspectral vegetation indices: modeling and validation," *Agr. Forest Meteorol.* **148**(8–9), 1230–1241 (2008), http://dx.doi.org/10.1016/j.agrformet.2008.03.005.
22. B. Demming-Adams and W. W. Adams, "The role of xanthophyll cycle carotenoids in the protection of photosynthesis," *Trends Plant Sci.* **1**(1), 21–26 (1996), http://dx.doi.org/10.1016/S1360-1385(96)80019-7.
23. J. J. Landsberg et al., "Energy conversion and use in forest: an analysis of forest production in terms of radiation utilization efficiency," H. L.Gholz, K. Nakane, and H. Shimoda, Eds., *The Use of Remote Sensing in the Modeling of Forest Productivity*, pp. 273–298, Kluver Academic Publishers, Dordrecht, The Netherlands(1996).
24. A. Young and G. Britton, "Carotenoids and stress," R. G.Alscher and J. R. Cummings, Eds., *Stress Responses in Plants: Adaptation and Aclimation Mechanisms*, pp. 87–112, Willey-Liss, New York (1990).
25. Z. Malenovský et al., "Scaling dimensions in spectroscopy of soil and vegetation," *Internat. J. App. Earth Ob. Geoinfo.* **9**(2), 137–164 (2007), http://dx.doi.org/10.1016/j.jag.2006.08.003.
26. R. Pu, P. Gong, and Q. Yu, "Comparative analysis of EO-1 ALI and Hyperion, and Landsat ETM+ data for mapping forest crown closure and leaf area index," *Sensors* **8**(6), 3744–3766 (2008), http://dx.doi.org/10.3390/s8063744.
27. D. R. Peddle et al., "Physically-based inversion modeling for unsupervised cluster labeling, independent forest classification and LAI estimation using MFM-5-scale," *Can. J. Re. Sens.* **33**(3), 214–225 (2007), http://dx.doi.org/10.5589/m07-026.
28. B. D. Ganapol et al., "LEAFMOD: a new within-leaf radiative transfer model," *Re. Sens. Envir.* **63**(2), 182–193 (1998), http://dx.doi.org/10.1016/S0034-4257(97)00134-X.
29. S. Jacquemoud and F. Baret, "PROSPECT: a model of leaf optical properties spectra," *Re. Sens. Envir.* **34**(2), 75–91 (1990), http://dx.doi.org/10.1016/0034-4257(90)90100-Z.
30. C. S. T. Daughtry et al., "Estimating corn leaf chlorophyll concentration from leaf and canopy reflectance," *Re. Sens. Envir.* **74**(2), 229–239 (2000), http://dx.doi.org/10.1016/S0034-4257(00)00113-9.

31. D. Haboudane et al., "Integrated narrow-band vegetation indices for prediction of crop chlorophyll content for application to precision agriculture," *Re. Sens. Envir.* **81**(2–3), 416–426 (2002), http://dx.doi.org/10.1016/S0034-4257(02)00018-4.
32. R. A. Jago, M. E. Cutler, and P. J. Curran, "Estimating canopy chlorophyll concentration from field and airborne spectra," *Re. Sens. Envir.* **68**(3), 217–224 (1999), http://dx.doi.org/10.1016/S0034-4257(98)00113-8.
33. W. Verhoef, "Light-scattering by leaf layers with application to canopy reflectance modeling–the SAIL model," *Re. Sens. Envir.* **16**(2), 125–141 (1984), http://dx.doi.org/10.1016/0034-4257(84)90057-9.
34. C. van der Tol et al., "An integrated model of soil-canopy spectral radiance observations, photosynthesis, fluorescence, temperature and energy balance," *Biogeosciences Disc.* **6**, 6025–6075 (2009), http://dx.doi.org/10.5194/bgd-6-6025-2009.
35. V. Demarez and J. P. Gastellu-Etchegorry, "A modeling approach for studying forest chlorophyll content," *Re. Sens. Envir.* **71**(2), 226–238 (2000), http://dx.doi.org/10.1016/S0034-4257(99)00089-9.
36. S. Jacquemoud, "Inversion of the PROSPECT + SAIL canopy reflectance model from AVIRIS equivalent spectra: theoretical study," *Re. Sens. Envir.* **44**(2–3), 281–292 (1993), http://dx.doi.org/10.1016/0034-4257(93)90022-P.
37. S. Chaurasia and V. K. Dadhwal, "Comparison of principal component inversion with VI-empirical approach for LAI estimation using simulated reflectance data," *Inter. ReJ. Sens.* **25**(14) 2881–2887 (2004), http://dx.doi.org/10.1080/01431160410001685018.
38. R. Houborg and E. Boegh, "Mapping leaf chlorophyll and leaf area index using inverse and forward canopy reflectance modeling and SPOT reflectance data," *Re. Sens. Envir.* **112**(1) 186–202 (2008), http://dx.doi.org/10.1016/j.rse.2007.04.012.
39. C. Atzberger, "Object-based retrieval of biophysical canopy variables using artificial neural nets and radiative transfer models," *Re. Sens. Envir.* **93**(2–3), 53–67 (2004), http://dx.doi.org/10.1016/j.rse.2004.06.016.
40. C. Atzberger et al., "Retrieval of wheat bio-physical attributes from hyperspectral data and SAILH + PROSPECT radiative transfer mode," M.Habermayer, A. Müller, and S. Holzwarth, Eds., in *Proc. of the 3rd EARSeL Workshop on Imaging Spectroscopy*, pp. 473–482, Herrchnig, Germany (2003).
41. Annual Tabular Overview, Air Quality Protection Division, Czech Hydrometeorological Institute, [on-line], http://portal.chmi.cz/files/portaldocs/uoco/tab_roc_CZ.html
42. P. J. Curran, W. R. Windham, and H. L. Gholz, "Exploring the relationship between reflectance red edge and chlorophyll concentration in slash pine leaves," *Tree Physiology* **15**(3), 203–206 (1995).
43. J. A. Gamon, J. Peñuelas, and C. B. Field, "A narrow-wave band spectral index that track diurnal changes in photosynthetic efficiency," *Re. Sens. Envir.* **41**(1), 35–44 (1992), http://dx.doi.org/10.1016/0034-4257(92)90059-S.
44. J. Peñuelas, F. Baret, and I. Fiella, "Semi-empirical indices to assess carotenoids/chlorophyll-a ratio from leaf spectral reflectance," *Photosynthetica* **31**(2), 221–230 (1995).
45. P. Rojík, "New stratigraphic subdivision of the tertiary in the Sokolov Basin in Northwestern Bohemia," *J. Czech Geological Society* **49**(3–4), 173–186 (2003).
46. P. Fabiánek, Forest Condition and Monitoring in the Czech Republic 1984–2003, Ministry of Agriculture of the Czech Republic and Forestry and Game Management Research Institute, ELAN spol. s.r.o., Přerov, Czech Republic, p. 431 (2004).
47. R. Porra, W. Thompson, and P. Kriedemann, "Determination of accurate extinction coefficients and simultaneous equations for assaying chlorophylls a and b extracted with four different solvents: verification of the concentration of chlorophyll standards by atomic absorption spectroscopy," *Biochimica et Biophysica Acta* **975**(3), 384–394 (1989), http://dx.doi.org/10.1016/S0005-2728(89)80347-0.
48. A. Welburn, "The spectral determination of chlorophyll-a and chlorophyll-b, as well as total carotenoids, using various solvents with spectrophotometers of different resolution," *J. Plant Phys.* **144**(3), 307–313 (1994), http://dx.doi.org/10.1016/S0176-1617(11)81192-2.

49. G. Schaepman-Strub et al., "Reflectance quantities in optical remote sensing—definitions and case studies," *Re. Sens. Envir.* **103**(1), 27–42 (2006), http://dx.doi.org/10.1016/j.rse.2006.03.002.
50. R. Richter, "Atmospheric/topographic correction for airborne imagery," ATCOR-4 User Guide, Version 5.0, January 2009, DLR-German Aerospace Centre, D-82234 Wessling, Germany, p. 168 (2009).
51. A. Berk, G. P. Anderson, and L. S. Bernstein, "MODTRAN-4 radiative transfer modeling for atmospheric correction, optical spectroscopic techniques and instrumentation for atmospheric and space research III book series," *Proc. SPIE* **3756**, 348–353 (1999).
52. J. Weyermann, A. Damm, and M. Schaepman, "Comparing empirical and semi-empirical approaches for brdf correction in airborne imaging," (in preparation)
53. J. Verrelst et al., "Angular sensitivity analysis of vegetation indices derived from CHRIS/PROBA data," *Re. Sens. Envir.* **112**(5), 2341–2351 (2008), http://dx.doi.org/10.1016/j.rse.2007.11.001.
54. C. B. Schaaf et al., "First operational BRDF, albedo nadir reflectance products from MODIS," *Re. Sens. Envir.* **83**(1–2), 135–148 (2002), http://dx.doi.org/10.1016/S0034-4257(02)00091-3.
55. D. Schläpfer, "Parametric Geocoding, PARGE Using Guide," Version 2.3, ReSe Applications Schläpfer & Remote Sensing Laboratories University of Zurich, PDF/CD-ROM Edition, Wil SG, p. 195
56. F. van der Meer and S. de Jong, "Quality control: signal to noise characterization," chapter 2, part 9, in *Imaging Spectrometry: Basic Principles and Prospective Application*, International Institute for Geo-information Science and Earth Observation (ITC), pp. 1922 (2002).
57. A. A. Green et al., "A transformation for ordering multispectral data in terms of image quality with implications for noise removal," *IEEE Trans. Geosci. Re. Sens.* **26**(1), 65–74 (1988), http://dx.doi.org/10.1109/36.3001.
58. D. A. Sims and J. A. Gamon, "Relationships between leaf pigment content and spectral reflectance across a wide range of species, leaf structures and developmental stages," *Re. Sens. Envir.* **81**(2–3), 337–354 (2002), http://dx.doi.org/10.1016/S0034-4257(02)00010-X.
59. E. Vogelmann, B. N. Rock, and D. M. Moss, "Red edge spectral measurements from sugar maple leaves," *Inter. J. Re. Sens.* **14**(8), 1563–1575 (1993), http://dx.doi.org/10.1080/01431169308953986.
60. J. G. P. Guyot and F. Baret, "Utilisation de la heute resolution spectrale pour suivre l'état des couverts végétaux," *Proceedings of the 4th International colloquium on spectral signatures of object in remote sensing*, ESA SP-287, Assois, France, 279–286 (1988).
61. Z. Malenovský et al., "A New hyperspectral index for chlorophyll estimation of a forest canopy: area under curve normalized to maximal band depth between 650–725 nm," *EARSel eProceedings* **5**(2), 161–172 (2006).
62. M. Schlerf et al., "Retrieval of chlorophyll content and nitrogen in Norway spruce (Picea abies KarstL.) using imaging spectroscopy," *Inter. J. Appl. Earth Ob. Geoinfo.* **12**(1), 17–26 (2010), http://dx.doi.org/10.1016/j.jag.2009.08.006.
63. R. I. Jennrich, "Stepwise regression," K.Enslein, A. Ralston, and S. Wilf, Eds., *Statistical Methods for Digital Computers*, pp. 76–90, Wiley, New York (1977).
64. R. N. Clark and T. L. Roush, "Reflectance spectroscopy: quantitative analysis techniques for remote sensing appélications," *J. Geo. Re.* **89**(B7), 6329–6340 (1984),http://dx.doi.org/10.1029/JB089iB07p06329.
65. P. K. Entcheva-Campbell et al., "Detection of initial damage in Norway spruce canopies using hyperspectral airborne data," *Inter. J. Re. Sens.* **25**(24), 5557–5583 (2004), http://dx.doi.org/10.1080/0143116041000172605.
66. S. S. Shapiro and M. B. Wilk, "An analysis of variance test for normality (complete samples)," *Biometrika* **52**(3–4), 591–611 (1965), http://dx.doi.org/10.1093/biomet/52.3-4.591.
67. D. M. Gates et al., "Spectral properties of plants," *Appl. Optic.* **4**(1), 11–20 (1965), .
68. W. Collins, G. L. Raines, and F. C. Canney, "Airborne spectroradiometer discrimination of vegetation anomalies over sulphide mineralization–a remote sensing technique," in *90th*

Annual Meeting problems and Abstracts, Geological Society of America Seattle, Vol. **9**, pp. 932–933, Washington, DC (1977).

69. N. H. Horler, J. Barber, and A. R. Barringer, "Effects of heavy metals on the absorbance and reflectance spectra of plants," *Inter. J. Re. Sens.* **1**(2), 121–136 (1980), http://dx.doi.org/10.1080/01431168008547550.
70. F. Boochs et al., "Shape of the red edge as vitality indicator for plants," *Inter. J. Re. Sens.* **11**(10), 1741–1753 (1990), http://dx.doi.org/10.1080/01431169008955127.
71. G. P. W. Clevers et al., "Derivation of the red edge index using MERIS standard band setting," *Inter. J. Re. Sens.* **23**(16), 3169–3184 (2002), http://dx.doi.org/10.1080/01431160110104647.
72. B. N. Rock, T. Hoshizaki, and J. R. Miller, "Comparison of in situ and airborne spectral measurement of the blue shift associated with forest decline," *Re. Sens. Envir.* **24**(1), 109–127 (1988), http://dx.doi.org/10.1016/0034-4257(88)90008-9.
73. D. N. H. Horler, M. Dockray, and J. Barber, "The red edge of plant leaf reflectance," *Inter. J. Re. Sens.* **4**(2), 279–288 (1983), http://dx.doi.org/10.1080/01431168308948546.
74. S. H. Chang and W. Collins, "Confirmation of the airborne biogeophysical mineral exploration technique using laboratory methods," *Econ. Geol. Bull. Soc. Econ. Geol.* **78**(4), 723–736 (1983), http://dx.doi.org/10.2113/gsecongeo.78.4.723.
75. J. A. Gamon, L. Serrano, and J. S. Surfus, "The photochemical reflectance index: an optical indicator of photosynthetic radiation use efficiency across species, functional types and nutrient levels," *Oecologia* **112**(4), 492–501 (1997), http://dx.doi.org/10.1007/s004420050337.
76. F. Thenot, M. Méthy, and T. Winkel, "The Photochemical Reflectance Index (PRI) as a water stress index," *Inter. J. Re. Sens.* **23**(23), 5135–5139 (2002), http://dx.doi.org/10.1080/01431160210163100.
77. L. Súarez et al., "Modeling PRI for water stress detection using radiative transfer models," *Re. Sens. Envir.* **113**(4), 730–744 (2009), http://dx.doi.org/10.1016/j.rse.2008.12.001.
78. C. Y. Kramer, "Extension of multiple range test to group means with unequal number of replications," *Biometrics* **12**(3), 307–310 (1956), http://dx.doi.org/10.2307/3001469.
79. ICP Forests Executive Report 2010, [on-line], http://icp-forests.net/page/icp-forests-executive-report
80. ICP Forests Manual, part XII Sampling and Analysis of Leaves and Needles, [on-line], http://icp-forests.org/pdf/FINAL_Foliage.pdf
81. C. W. Woodal et al., "Status and future of the forest health indicators program of the USA," *Environ. Monit. Assess.* **177**(1–4), 419–436 (2011), http://dx.doi.org/10.1007/s10661-010-1644-8.
82. J. Soukupová, B. N. Rock, and J. Albrechtová, "Comparative study of two spruce species in a polluted mountainous region," *New Phytologist* **150**(1), 133–145 (2001), http://dx.doi.org/10.1046/j.1469-8137.2001.00066.x.
83. J. Oleksyn et al., "Growth and physiology of Picea abies populations from elevational transects: common garden evidence for altitudinal ecotypes and cold adaptation," *Funct. Ecol.* **12**(4), 573–590 (1998), http://dx.doi.org/10.1046/j.1365-2435.1998.00236.x.
84. D. Barsi et al., "Generic variation and control of chloroplast pigment concentrations an related needle-level traits in Picea rubens, Picea marina and their hybrids: moisture and light environmental effects," *Trees—Struct. Funct.* **23**(3), 555–571 (2009), http://dx.doi.org/10.1007/s00468-008-0301-0.
85. D. Siefermannharms, "Light and temperature control of season-dependent changes in the alpha-carotene and beta-carotene content of spruce needles," *J. Plant Phys.* **143**(4–5), 488–494 (1994).
86. C. Atzberger and W. Werner, "Needle reflectance of healthy and diseased Spruce stands," *1st EARSeL Workshop on Imaging Spectroscopy*, pp. 271–283, Remote Sensing Laboratories, University of Zurich, Impression Dumas, Saint-Etiene rance (1998).

Biographies and photographs of the authors are not available.